

Zener Tunneling of Light Waves in an Optical Superlattice

Mher Ghulinyan,^{*} Claudio J. Oton,[†] Zeno Gaburro, and Lorenzo Pavesi

Department of Physics, University of Trento and INFM, via Sommarive 14, I-38050 Povo (Trento), Italy

Costanza Toninelli[‡] and Diederik S. Wiersma

European Laboratory for Nonlinear Spectroscopy and INFM-MATIS, via Nello Carrara 1, 50019 Sesto Fiorentino (Florence), Italy

(Received 23 July 2004; published 30 March 2005)

We report on the observation of Zener tunneling of light waves in spectral and time-resolved transmission measurements, performed on an optical superlattice made of porous silicon. The structure was designed to have two photonic minibands, spaced by a narrow frequency gap. A gradient in the refractive index was introduced to create two optical Wannier-Stark ladders and, at a critical value of the optical gradient, tunneling between energy bands was observed in the form of an enhanced transmission peak and a characteristic time dependence of the transmission.

DOI: 10.1103/PhysRevLett.94.127401

PACS numbers: 78.67.Pt, 42.25.Dd, 42.70.Qs, 73.21.Cd

Electrical Zener breakdown is an intriguing topic among the various transport phenomena of charge carriers in solids. The phenomenon was originally described in 1934 by Zener [1]: in the presence of a large electric field on a crystal, direct tunneling of a Bloch particle into a continuum of states of another energy band takes place without extra energy. This *nonresonant* Zener tunneling is the main reason for electrical breakdown in reverse-biased diodes. On the other hand, *resonant* Zener tunneling is possible at high electric fields between charge carriers in Wannier-Stark ladders (WSL). A WSL consists of a set of equidistant states which are confined in space [2]. In a crystal that is exposed to a stationary electric field, these states form the energy spectrum of a Bloch particle. The advent of electronic superlattices [3] opened up new possibilities to study dynamical interference phenomena on time scales shorter than the electron decoherence time. Recent experimental results include the observation of WSLs [4], Zener breakdown [5], and Bloch oscillations [6]. Resonant tunneling between the anticrossing Wannier-Stark states of neighboring energy minibands has been considered theoretically [7] and observed in experiments [8].

The wave nature of both electrons and photons is the basis of important analogies between electron transport phenomena in solids and light propagation in complex dielectric materials [9]. Electronic crystals have an optical analogue in the form of photonic crystals [10] and several electron transport phenomena, like the Hall effect, weak and strong localization, and conductance fluctuations were observed to exist also for optical waves [11]. The use of light waves instead of electrons has the advantage that particle-particle interactions can be neglected, which allows one to isolate the pure interference effects. The existence of the optical counterpart of a WSL was discussed theoretically [12] and observed experimentally in linearly chirped Moiré gratings [13]. One-dimensional optical superlattices can be realized in the form of dielectric multilayer structures and constitute the optical analogue of

electronic superlattices. The role of the electric field is played here by an optical thickness gradient $\Delta\delta$ along the multilayer growth direction, which introduces, to first order, a linear tilt of the photonic miniband. Optical Bloch oscillations have recently been observed in time-resolved transmission experiments on an optical superlattice with gradient [14].

In this Letter we report on the experimental observation of Zener tunneling of light waves in spectral and time-resolved transmission measurements. Optical superlattices of porous silicon were designed to have a refractive index gradient such that two WSLs were formed. By comparing the behavior of different superlattices with increasing optical gradient, we were able to observe resonant coupling of two Wannier-Stark states leading to delocalization of the optical waves and hence resonant Zener tunneling.

A one-dimensional optical superlattice can be constructed by stacking two dielectric layers (say, *A* and *B*) with refractive indices n_A and n_B , in such a way that Bragg reflector sequences (i.e., *BABABAB*) and cavity sequences (i.e., *AA*) are alternated [15]. Such a superlattice exhibits narrow transmission bands, called minibands. The longest-wavelength (first order) miniband is centered around a wavelength λ_c if the optical thickness of layers *A* and *B* equals $\lambda_c/4$. One can form a superlattice with a double series of minibands by alternating two different types of cavities formed by layers *C* and *D*. This leads to the following sequence: *BABABAB* (*CC*)₁ *BABABAB* (*DD*)₁ ... (*CC*)_{*m*} *BABABAB* (*DD*)_{*m*} *BABABAB*. The central wavelength of the lowest order miniband of each series can be chosen by changing the refractive index and thickness of the layers *C* and *D*. We designed our samples such that the central wavelengths of the minibands associated with the cavities *CC* and *DD* are at $\lambda_1 = 0.81\lambda_c$ and $\lambda_2 = 0.96\lambda_c$, respectively, with $\lambda_c = 1702$ nm. In practice, $m = 6$, so that six cavities of type *CC* and *DD* are alternated and coupled through *BABABAB* Bragg mirrors.

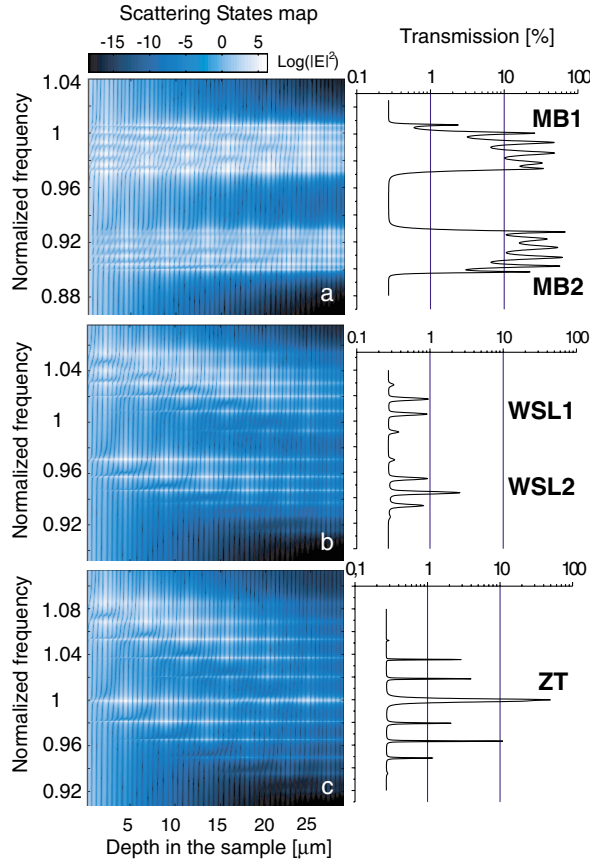


FIG. 1 (color online). Transfer matrix calculation for the intensity distribution of the light inside the sample. The intensity is plotted as a color scale versus the normalized frequency ω/ω_0 and depth inside the sample, with $\omega_0 = 192.3$ THz. (a) Flat miniband situation, $\Delta\delta = 0\%$, (b) optical WSLs, $\Delta\delta = 6.7\%$, (c) resonant Zener tunneling (ZT), $\Delta\delta = 10.3\%$. The calculated transmission spectra are shown in the right panels (a slight offset of 0.27% is used to allow for the use of a logarithmic scale). The blueshift of the spectral features with increasing gradient is due to the reduced optical thickness of the layers.

The distribution of the light intensity inside this superlattice structure can be calculated using a transfer matrix method [16]. The results of this calculation for the above structure are shown in Fig. 1. The transmission spectra are shown in a logarithmic scale on the right-hand side of the graphs. The parameters used in the calculations correspond to those of the samples studied in the actual experiment. The calculated spectra also take into account the loss coefficient of 93 cm^{-1} of the samples (due to absorption and scattering out of the propagation axis) which gives a nearly negligible spectral broadening of the transmission peaks of 0.3–0.5 nm. From the calculated intensity distributions we can see that in the absence of a refractive index gradient indeed two flat minibands MB1 and MB2 are formed separated by a minigap [Fig. 1(a)]. The central frequencies of the minibands are $\omega_1 = 217$ THz and $\omega_2 = 182.8$ THz.

The introduction of a gradient in the refractive index tilts the photonic bands of the superlattice. In Fig. 1(b) the superlattice with 6.7% negative gradient is shown (for technical reasons, the gradient is defined with reference to the last layer). In this case the optical WSLs can be appreciated in the form of spatially confined discrete modes leading to equidistant peaks in the transmission measurement. This spatial confinement of the optical modes causes a decrease of absolute transmission value from 50% in the flat band case (delocalized states) down to 2% for the transmission peaks in the WSL. At a *critical* gradient value an anticrossing between the last state of MB1 and the first one of MB2 occurs. Coupling induced delocalization of these states takes place, which appears as an intense resonant tunneling channel [Fig. 1(c)] and an enhanced transmission peak of 42%.

We have grown these optical superlattices by controlled electrochemical etching of heavily doped *p*-type (100)-oriented silicon. Different etching current densities were used to grow each type of layer (50 mA/cm² for *A*, *C*, and *D* layers and 7 mA/cm² for layer *B*). An etch stop was used at the end of the growth of each layer to allow etchant recycling. The refractive indices were $n_A = n_C = n_D = 1.5$ and $n_B = 2.12$. The physical thickness of the layers was controlled by adjusting the duration of the etch times and are approximately $d_A = 283$ nm, $d_B = 200$ nm, $d_C = 230$ nm, and $d_D = 273$ nm. The superlattice structures were made freestanding by applying an electropolishing current pulse at the end of the growth process. (See Ref. [15] for more details.)

A negative optical thickness gradient was achieved by changing the duration of the etch stop current, which controls the refractive index and, therefore, the optical thickness of each layer. We produced samples with controlled gradient values in the range from $\Delta\delta = 0$ to 18%. These $\Delta\delta$ values were confirmed by comparison of calculated and measured transmission spectra. Transmission spectra of the samples were measured between 900 to 2200 nm with a spectrophotometer and a collimated beam with 1 mm spot diameter (wavelength resolution of 2 nm). It is known that porous silicon samples suffer from lateral inhomogeneities due to doping variations of the Si wafers, which lead to an inhomogeneous widening of the transmission peaks measured with broad beams [15]. For this reason some spectra were measured in a high-resolution transmission setup with a very small numerical aperture (NA ~ 0.0075 , leading to a negligible broadening of 0.02 nm at 1550 nm wavelength), where a tunable laser source focused to a 35 μm diameter spot was used.

In Fig. 2 the transmission spectra of optical superlattices with different values of $\Delta\delta$ are shown. Figures 2(a)–2(c) show the wide range spectra, while in 2(d)–2(f) zooms around ω_0 are shown. In a flat band situation [2(a) and 2(d)] two minibands are observed, which are separated by a minigap with negligible transmission. In Fig. 2(e) one can

observe that the introduction of a gradient (here 6.7%) leads to the formation of an optical WSL in both minibands. These are observed as narrow (but relatively weak) transmission peaks. At a certain critical gradient, the two WSLs start to couple within the physical extension of the superlattice. In our samples this happens at a gradient of $\Delta\delta \sim 10.3\%$. An anticrossing of the edge states occurs in this case and resonant Zener tunneling takes place, which is observed as an intense peak in the transmission spectrum [2(c) and 2(f)]. This observation, together with the calculation in Fig. 1, nicely demonstrates the physics of resonant Zener tunneling. An efficient transmission channel opens when two internal resonances inside the sample couple to form a delocalized mode of which the transmission coefficient is much larger than the sum of the transmission coefficients of the two individual resonances before coupling. Such internal resonances can couple only if the frequency difference between the modes is smaller than their bandwidth. The characteristic property of Zener tunneling is that this frequency difference is tuned by changing the gradient inside the sample and that the internal resonances arise from a double WSL.

To examine the Zener tunneling regime in detail, we grew a superlattice with a refractive index gradient that depended on the lateral position of the incident beam on the sample. This way the gradient could be changed from 6.5% to 10.7% by simply scanning the sample in a lateral direction. Figure 3 shows the measured high-resolution transmission spectra taken at different points corresponding to different gradients. In the vicinity of the threshold gradient the transmission spectrum is extremely sensitive to small changes of the optical path. One can see how the edge states of the two WSLs start to overlap, and the saddlelike curvature transforms gradually into a sharp resonance of 42% transmission. In the inset of Fig. 3 the

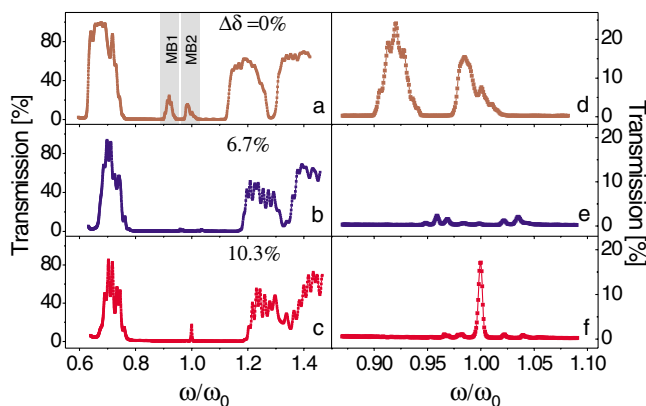


FIG. 2 (color online). Transmission spectra of the optical superlattices: (a) flat band situation $\Delta\delta = 0\%$, (b) $\Delta\delta = 6.7\%$, (c) $\Delta\delta = 10.3\%$. (d)–(f) A zoom of the wide range spectra around the miniband region. Resonant Zener tunneling is observed in (c) and (f) as an enhanced transmission peak in the center of the minigap.

calculated transmission values at ω_0 for $\Delta\delta$ in the range 0%–25% are compared with the experimental data. The analysis of these spectra shows that, together with the increase of the transmission value, this resonant transmission peak gets wider. At resonance its full width half maximum (FWHM) is about 4.1 nm, whereas the width of the uncoupled WSL peaks at $0.98\omega_0$ and $1.025\omega_0$ is about 2 nm. This broader non-Lorentzian line shape is the effect of repulsion between the two coupled resonances.

The line shape differences are difficult to appreciate even in the high precision spectra, due to the narrow widths of the peaks. The effect should be observable, however, in the time domain. A single resonance corresponds to a phase shift of π , which results in an asymmetric pulse shape with single exponential decay at long times. A double resonance mode experiences a different phase versus frequency dependence, which affects the shape of the time response, namely, shifting its maximum towards longer times. This feature should allow one to distinguish among peaks of the same width, originating from resonances of different multiplicity.

To test these properties we performed time-resolved pulse transmission experiments on our samples. We employed an optical gating technique as described in Ref. [14]. The gate beam was obtained from a mode-locked Ti:sapphire laser centered at a wavelength of 810 nm and with 130 fs pulse duration (bandwidth about 8 nm). The probe beam was obtained from a synchronously pumped Optical Parametric Oscillator (Spectraphysics OPAL), with a central wavelength tunable between 1400 and 1600 nm. The transmitted signal through the sample was

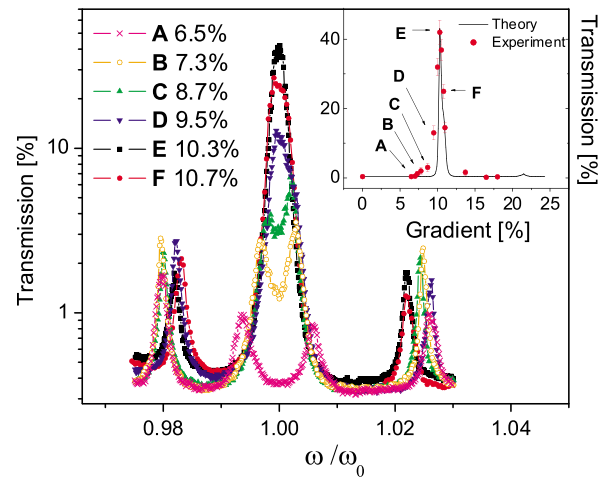


FIG. 3 (color online). Transmission spectra of a tilted superlattice around the value of the refractive index gradient where the first anticrossing of the optical WSLs and hence Zener tunneling occurs. The transmission is plotted on a logarithmic scale. The inset shows a comparison between the experimental transmission values of the maximum transmission around the central frequency ω_0 as a function of the gradient and the transfer matrix calculations.

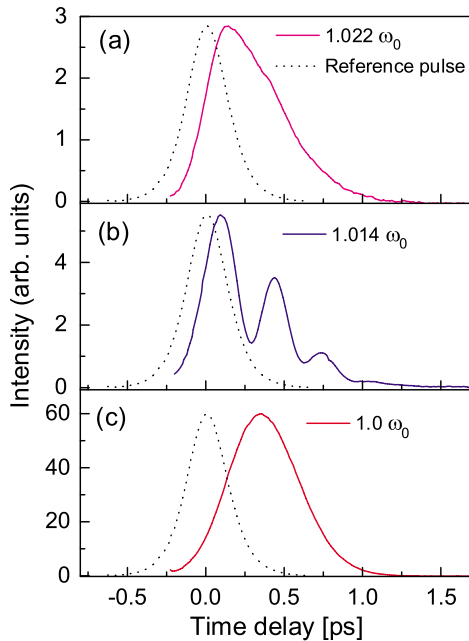


FIG. 4 (color online). Time-resolved transmitted signals from a double superlattice with refractive index gradient in the Zener tunneling regime. (a), (b), and (c) correspond to different probe wavelengths. In (a) a single resonance is excited, whereas in (b) the WSL is excited leading to (damped) Bloch oscillations. In (c) the Zener tunneling peak is excited leading to a strongly delayed but nearly symmetric transmitted pulse. The dotted curves refer to the transmission in the absence of a sample.

mixed with the gate beam in a 0.3 mm thick nonlinear crystal (beta barium borate) to obtain sum frequency generation. The gate pulse experienced a time delay via a variable delay line, and a standard lock-in technique was used to suppress noise.

The observed behavior is shown in Fig. 4. When a single state is excited [4(a)], light is spatially confined in a single resonance. In this case the intensity simply decays exponentially with a time constant approximately (within the spectral resolution) given by the inverse of the spectral width of the resonance. A more complex behavior is found when two modes of the WSL are excited [4(b)]. Here the transmitted pulse oscillates with a period of 200 fs, determined by the energy difference between the levels of the WSL. These are the known time-resolved Bloch oscillations. Finally, Fig. 4(c) shows the transmitted signal when the input beam is centered at 1560 nm, around the Zener tunneling peak of Fig. 3. The time-resolved profile does not have the typical shape of a single resonance. It is characterized by a more rapid decay and a substantial delay of the top of the pulse. The faster decay time is due to the stronger coupling of the mode with the sample environment. The delay is caused by the transient time necessary to build up the double resonance of the Zener tunneling mode.

In conclusion, we have reported the optical analogue of Zener tunneling. The observation has been performed via

spectral and time-resolved transmission measurements on specifically designed optical superlattices, which exhibit two minibands. A controlled refractive index gradient along the light propagation direction in the superlattice was used to tilt the photonic band structure. At a critical gradient value, coupling of photonic minibands occurs, resulting in delocalization of the optical Wannier-Stark states and consequently Zener tunneling of the light waves.

We thank J.H. Korsch for suggesting the analogy with electronic Zener tunneling, J. Pendry and V. Freilikher for discussions, and R. Sapienza, P. Costantino, and S. Gottardo for help with the time-resolved experiments and discussions. This work was financially supported by the INFM FIRB and RANDES, MIUR Cofin 2002, and PRIN 2004 projects.

*Electronic addresses: mghool@science.unitn.it;
www.science.unitn.it/~semicon/

†Present address: Departamento de Física Basica,
University of La Laguna, Avda. Astrofísico Fco.
Sánchez s/n, La Laguna 38204 Tenerife, Spain.

‡Electronic addresses: toninelli@lens.unifi.it;
www.complexphotonics.org

- [1] C. Zener, Proc. R. Soc. London A **145**, 532 (1934).
- [2] G.H. Wannier, Phys. Rev. **100**, 1227 (1955).
- [3] L. Esaki and R. Tsu, IBM J. Res. Dev. **14**, 61 (1970).
- [4] E.E. Mendez, F. Agullo-Rueda, and J.M. Hong, Phys. Rev. Lett. **60**, 2426 (1988).
- [5] H. Schneider *et al.*, Phys. Rev. Lett. **65**, 2720 (1990); B. Rosam *et al.*, Phys. Rev. Lett. **86**, 1307 (2001).
- [6] T. Dekorsy *et al.*, Phys. Rev. B **50**, 8106 (1994); V.G. Lyssenko *et al.*, Phys. Rev. Lett. **79**, 301 (1997); T. Hartmann *et al.*, New J. Phys. **6**, 2 (2004).
- [7] S. Glutsch and F. Bechstedt, Phys. Rev. B **60**, 16 584 (1999).
- [8] B. Rosam *et al.*, Phys. Rev. B **68**, 125301 (2003).
- [9] *Photonic Crystals and Light Localization in the 21st Century*, edited by C.M. Soukoulis, NATO Advanced Study Institutes, Ser. C Vol. 563 (Kluwer, Dordrecht, 2001).
- [10] J.D. Joannopoulos, R.D. Meade, and J.N. Winn, *Photonic Crystals* (Princeton University Press, Princeton, NJ, 1995).
- [11] Ping Sheng, *Introduction to Wave Scattering, Localization, and Mesoscopic Phenomena* (Academic Press, New York, 1995); *Wave Scattering in Complex Media, from Theory to Applications*, edited by S.E. Skipetrov and B.A. van Tiggelen, NATO Advanced Study Institutes, Ser. II Vol. 107 (Kluwer, Dordrecht, 2003).
- [12] G. Monsivais, M. del Castillo-Mussot, and F. Claro, Phys. Rev. Lett. **64**, 1433 (1990).
- [13] C. Martijn de Sterke *et al.*, Phys. Rev. E **57**, 2365 (1998).
- [14] R. Sapienza *et al.*, Phys. Rev. Lett. **91**, 263902 (2003).
- [15] M. Ghulinyan *et al.*, J. Appl. Phys. **93**, 9724 (2003).
- [16] J.B. Pendry, Adv. Phys. **43**, 461 (1994).